附件

中 國 醫 藥 大 學

專題研究計畫成果報告

計畫名稱：建立長循環性奈米鈣油體之技術平台

計畫編號：CMU 100- S - 29

執行期限： 101 年 8 月 31 日至 102 年 7 月 31 日

單位名稱：醫技系

主持人：姜中人

中 華 民 國 102 年 7 月 31 日

Appl Microbiol Biotechnol
DOI 10.1007/s00253-011-3716-2

BIOTECHNOLOGICAL PRODUCTS AND PROCESS ENGINEERING

Caleosin-assembled oil bodies as a potential delivery nanocarrier

Chung-Jen Chiang · Shen-Chuan Lin · Li-Jen Lin · Chih-Jung Chen · Yun-Peng Chao

Received: 7 September 2011 / Revised: 25 October 2011 / Accepted: 6 November 2011

Abstract Encapsulation of hydrophobic agents with nanocarriers is challenging. Therefore, we have sought to use nanoscale artificial oil bodies (NOBs) as an alternative delivery carrier. To constitute NOBs, caleosin (Cal), a structural protein of plant seed oil bodies, was first fused with ZH2 (Cal-ZH2). ZH2 is a bivalent anti-HER2/*neu* affibody with a high affinity towards the HER2/*neu* receptor. After overproduction in *Escherichia coli*, insoluble Cal-ZH2 was isolated and used to assemble NOBs in one step. Consequently, resulting NOBs had a zeta potential around −49 mV and ranged in size from 150 to 200 nm. Upon loading with a hydrophobic fluorescence dye, NOBs were found to be selectively internalized into HER2/*neu*-positive tumor cells. Further analyses showed that more than 90% cells were invaded by dye-loaded NOBs and the cargo dye was released in cells with time. In addition, the in vitro assay revealed the release of the dye from NOBs in a slow and prolong manner. Overall, these results indicate the potential of Cal-based NOBs as a delivery vehicle.

Keywords Artificial oil body · Caleosin · Targeted delivery · HER2/*neu*

C.-J. Chiang (✉) · S.-C. Lin · C.-J. Chen
Department of Medical Laboratory Science and Biotechnology,
China Medical University,
91 Hsue-Shih Road,
Taichung 40402, Taiwan
e-mail: cjchiang@mail.cmu.edu.tw

L.-J. Lin
School of Chinese Medicine, China Medical University,
Taichung, Taiwan

Y.-P. Chao (✉)
Department of Chemical Engineering, Feng Chia University,
100 Wen Hwa Road,
Taichung 40424, Taiwan
e-mail: ypchao@fcu.edu.tw

Introduction

Plant seeds are rich in oil bodies (OBs) that provide the fuel for seedling growth (Huang 1996; Napier et al. 1996). OBs consist of a triacylglycerol (TAG) matrix surrounded by a monolayer of structural protein-bound phospholipids (PLs). Oleosin (Ole) is recognized as the prominent structural protein associated with OBs (Frandsen et al. 2001b). This protein has a central hydrophobic region along with two hydrophilic domains. One domain is embedded in TAG matrix while the other domain protrudes outwards. The negative charge of these two terminal domains provides OBs with the electronegative repulsion that prevents OBs from coalescence. This, in turn, results in the stability of OBs in the form of separate entities both in vivo and in vitro, and the size of OBs can reach 0.5–2 μm in diameter on average (Tai et al. 2002).

OBs can be reconstituted in vitro to form artificial oil bodies (AOBs). This is carried out by subjecting TAG, PLs, and structural proteins to sonication (Tzen et al. 1992, 1998). Ole is the structural protein that has been primarily employed for assembling AOBs (Peng et al. 2003). The resulting AOBs are comparable in size, topology, and stability to those of isolated seed OBs (Tzen and Huang 1992). These unique structural and topological features of Ole-based AOBs have

Published online: 30 November 2011

found many biotechnological applications, such as the scaffold-assisted refolding and purification of recombinant proteins (Chiang et al. 2005, 2007; Peng et al. 2004), one-step immobilization of enzymes (Chiang et al. 2006), and cargo delivery (Chiang et al. 2010, 2011).

One promising approach to effectively combat cancers is to employ carriers to selectively deliver drugs to tumor sites (Farokhzad and Langer 2009). This approach relies on a drug-loaded carrier conjugated with a bioactive ligand that recognizes the biomarker of tumor cells. Consequently, a sufficient dose of chemotherapeutic drugs can reach cancerous loci, thereby minimizing the detrimental side effect of drugs toward normal cells (Cho et al. 2008). However, many potent anticancer pharmaceuticals are poorly soluble. Oral or intravenous administration of hydrophobic agents usually leads to low bioavailability of pharmaceuticals due to the aggregate deposition at local sites (Fernandez et al. 2001; Lipinski et al. 2000). Accordingly, various drug carrier systems have been proposed to address this issue, including liposomes (Andresena et al. 2005), synthetic polymers (Zhang et al. 2008), micelles (Torchilin 2005), and others (Cohen and Bernstein 1996). Nevertheless, many technical difficulties need to be overcome before an effective formulation of water-repelling agents is developed (Torchilin 2007).

In principle, an effective drug carrier must be small, biocompatible, and biodegradable. AOBs, consisting of natural biomaterials, apparently hold these characteristics. Recently, we have explored the feasibility of AOBs for targeted delivery of hydrophobic agents (Chiang et al. 2010, 2011). By tailoring the ratio of Ole to oil, nanoscale AOBs (NOBs) could be obtained. Ole was fused with a small bioactive domain, either the arginine–glycine–aspartate (RGD) motif or the bivalent anti-HER2/*neu* affibody (denoted as ZH2). The resulting fusion genes were overexpressed in *Escherichia coli* and the hybrid proteins were isolated for constitution of NOBs. To illustrate, a hydrophobic dye was encapsulated into NOBs that displayed RGD or ZH2 motif on the surface. Upon administration, the RGD- and ZH2-displayed NOBs were selectively internalized into $\alpha_v\beta_3$ integrin- and HER2/*neu*-positive tumor cells, respectively. The internalization efficiency could reach 80% in both cases as revealed by the flow cytometry analysis. Moreover, NOBs entered tumor cells via the endosomal entry pathway and disintegrated with time in response to the low pH condition. The cargo dye was then released into cell cytoplasm. Overall, the results indicate a new application of NOBs in the field of cancer nanotechnology.

Caleosin (Cal) is another structural protein associated with seed OBs (Chen et al. 1999). The structure of Cal is very similar to that of Ole (Frandsen et al. 2001a). A previous study found that AOBs reconstituted with Cal had a smaller size and exhibited higher stability relative to those with Ole (Liu et al. 2009). Therefore, it was intriguing to examine the feasibility of Cal-based NOBs for targeted delivery of insoluble agents. To this end, Cal was fused with ZH2 (Cal-ZH2). A single domain of ZH2 consists of 58 amino acid residues and exhibits a high binding affinity towards the extracellular domain of HER2/*neu* (Orlova et al. 2006). After overproduction in *E. coli*, Cal-ZH2 was isolated and used to assemble NOBs with the size ranging between 150 and 200 nm. By encapsulation with a hydrophobic dye, Cal-based NOBs were shown to selectively penetrate HER2/*neu*-positive tumor cells in an effective way. Moreover, the cargo dye was released from the pH-responsive nature of Cal-based NOBs upon internalization. The result indicates the potential of Cal-based NOBs as a delivery carrier.

Materials and methods

Plasmid construction

The ZH2 motif comprises two identical domains of $Z_{HER2:342}$ (Orlova et al. 2006). It was synthesized by Mission Biotech. Co. (Taiwan) and then subcloned into plasmid pBluescript-SKII (Stratagene Co., USA) to obtain plasmid pBlue-ZH2 (Chiang et al. 2011). The ZH2 motif was recovered from plasmid pBlue-ZH2 with *Eco*RV-*Hin*dIII digestion and incorporated into plasmid pET29a-Cal (Chen et al. 2004) to give plasmid pJO1-Cal-ZH2. This plasmid contains the ZH2 domain fused to the C terminus of Cal and the fusion gene is under the control of the T7 promoter. In contrast, plasmid pET29a-Cal contained Cal alone.

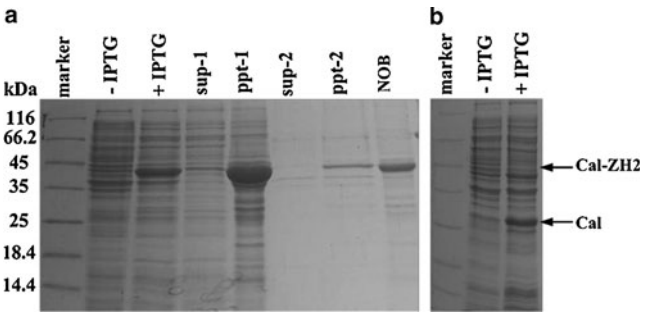

Fig. 1 SDS-PAGE analyses of Cal-ZH2 production in *E. coli*. *E. coli* strain bearing plasmid pJO1-Cal-ZH2 (*left panel*) or pET29a-Cal (*right panel*) was cultured and induced (+IPTG) for protein production. By centrifugation, proteins of plasmid pJO1-Cal-ZH2-bearing bacteria were fractioned into the soluble part (*sup-1*) and insoluble part (*ppt-1*). Insoluble Cal-ZH2 was used for assembly of NOBs with two fractions left after centrifugation, including the supernatant (*sup-2*) and precipitate (*ppt-2*). NOBs were recovered from the top of the solution and heated to release the protein (AOB)

Protein overproduction

E. coli strain BL21(DE3) was transformed with plasmid pJO1-Cal-ZH2 and pET29a-Cal. These plasmid-bearing bacterial strains were grown in Luria–Bertani (LB) medium (Miller 1972) at 37°C. To induce protein production, 100 μM Isopropyl β-D-1-thiogalactopyranoside (IPTG) was added to the culture medium. After induction for 4 h, bacteria were harvested by centrifugation and resuspended in 1 ml of 0.01 M sodium phosphate buffer (pH 7.5). Sulfate-polyacrylamide gel electrophoresis (SDS-PAGE) was then conducted to analyze the proteins as previously reported (Chiang et al. 2008).

Self-assembly of NOBs

NOBs were assembled essentially following the previous method (Chiang et al. 2005). In brief, unless stated otherwise the assembly solution (1 ml) consisted of 100 μg olive oil, 150 μg PLs, and 500 μg Cal-ZH2 or Cal in 10 mM sodium phosphate buffer (pH 7.5). The plant oils used here were soybean oil (Taiwan Sugar Co., Taiwan), peanut oil (Leader Price Co., Taiwan), sesame oil (Taisun Co.), olive oil (Taisun Co.), and mineral oil (Sigma, USA). The solution was then subjected to sonication for 10 s with the amplitude set at 20%. Upon centrifugation, NOBs were removed from the top of the solution. To encapsulate the cargo agent into

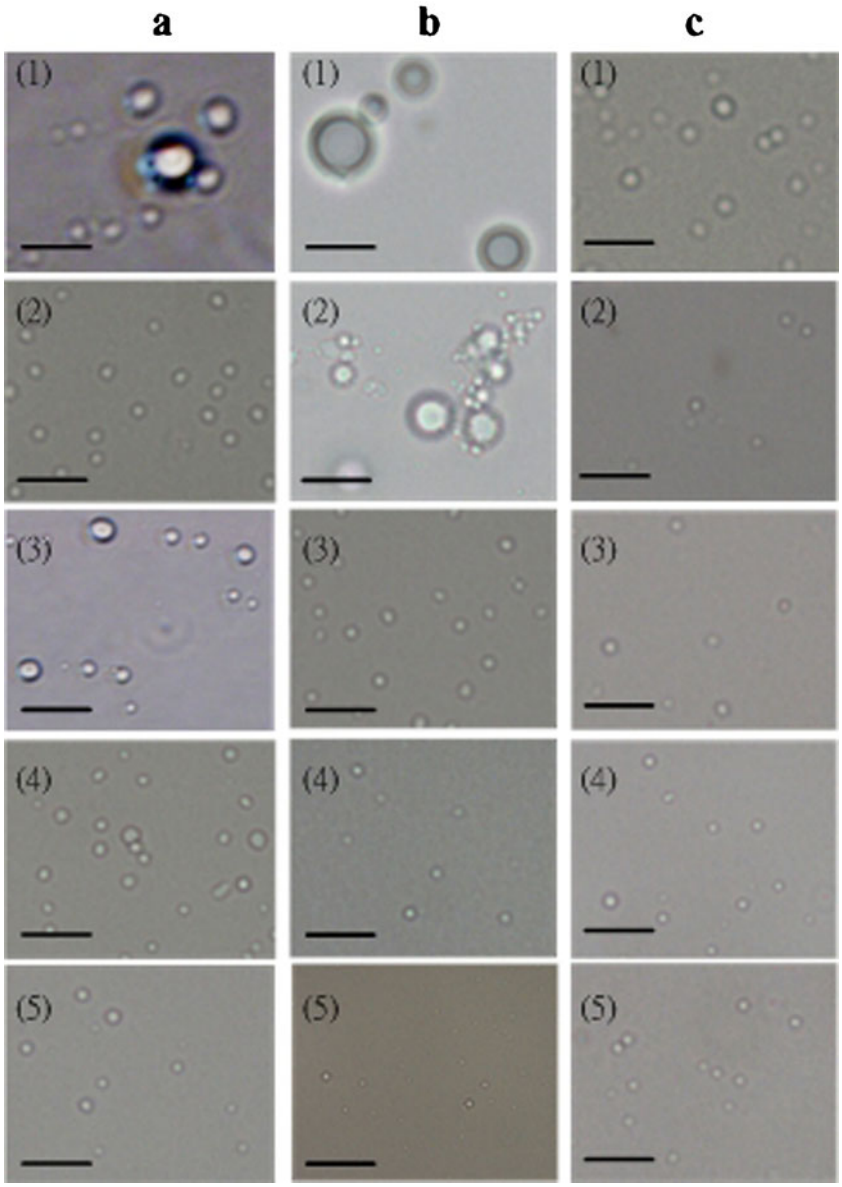

Fig. 2 Morphology of Cal-based NOBs at various conditions. Morphology of Cal-based NOBs was analyzed by light microcopy. **a** Assembly of Cal-based NOBs with various plant oils, including (*1*) mineral oil, (*2*) peanut oil, (*3*) soybean oil, (*4*) olive oil, and (*5*) sesame oil. **b** Assembly of Cal-based NOBs with various O/P ratios at (*1*) 10:1, (*2*) 2:1, (*3*) 1:1, (*4*) 1:5, and (*5*) 1:10. **c** Assembly of Cal-based NOBs at pH (*1*) 6.5, (*2*) 7.0, (*3*) 7.5, (*4*) 8.0, and (*5*) 9.0. Scale bar=2 μm

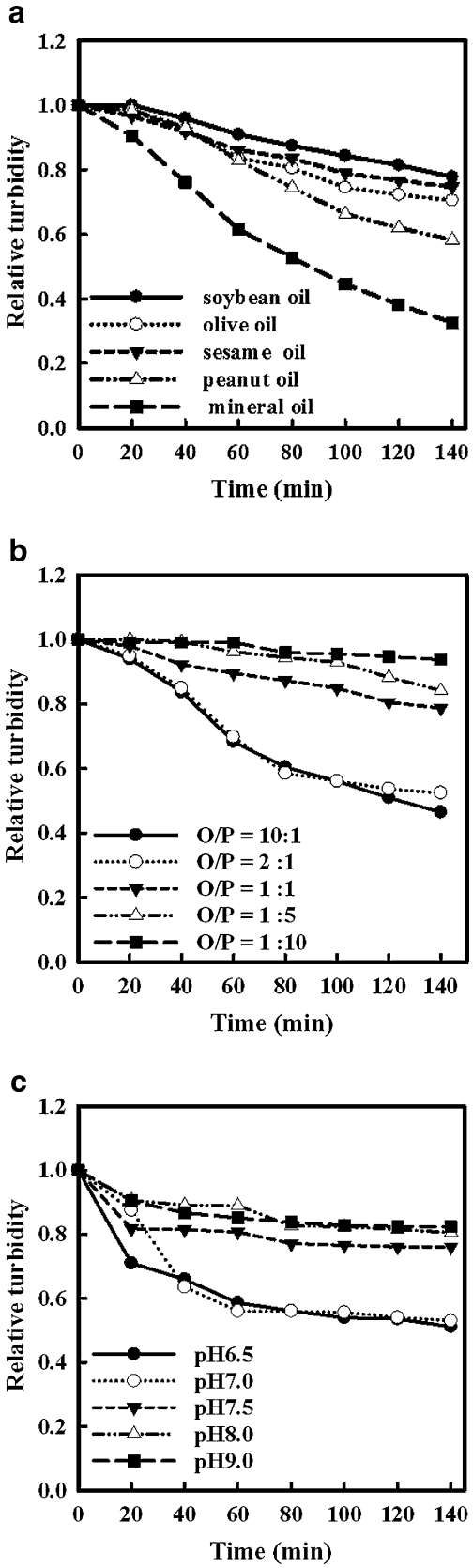

Fig. 3 Stability of Cal-based NOBs at various conditions. The stability of NOBs was determined by the turbidity test as described. **a** Stability profile of NOBs assembled with various types of oils. **b** Stability profile of NOBs assembled at various O/P ratios. **c** Stability profile of NOBs assembled at various pHs

NOBs, 1 μg yellow GGK dye (Widetex Co., Taiwan) was added to the assembly solution.

Morphology, size, and stability of NOBs

According to a previous report (Chiang et al. 2010), the morphology and size of NOBs were analyzed with a light microscope (Nikon type E600, Japan) and a particle size analyzer (Beckman Coulter, USA), respectively. The stability of NOBs was determined by the turbidity test as reported previously (Chiang et al. 2010). In addition, dye-loaded NOBs were analyzed by atomic force microscopy (AFM) with the NS4/D3100CL/Multi Mode (Digital Instrument, Germany). A drop of the suspension containing NOBs was overlaid onto the mica surface at room temperature. A cantilever was employed to scan the sample with a nominal force constant of 20 Nm^{-1}.

Cell culture

Cell cultures were maintained following the protocol described by Chiang et al. (2011). The human tumor cell

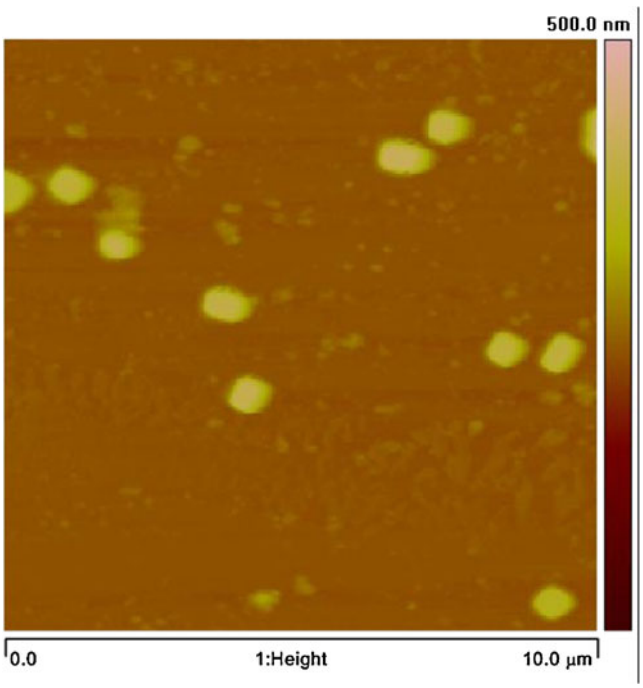

Fig. 4 Morphology of NOBs by AFM. NOBs were assembled with the O/P ratio at 1:5 and at pH 7.5

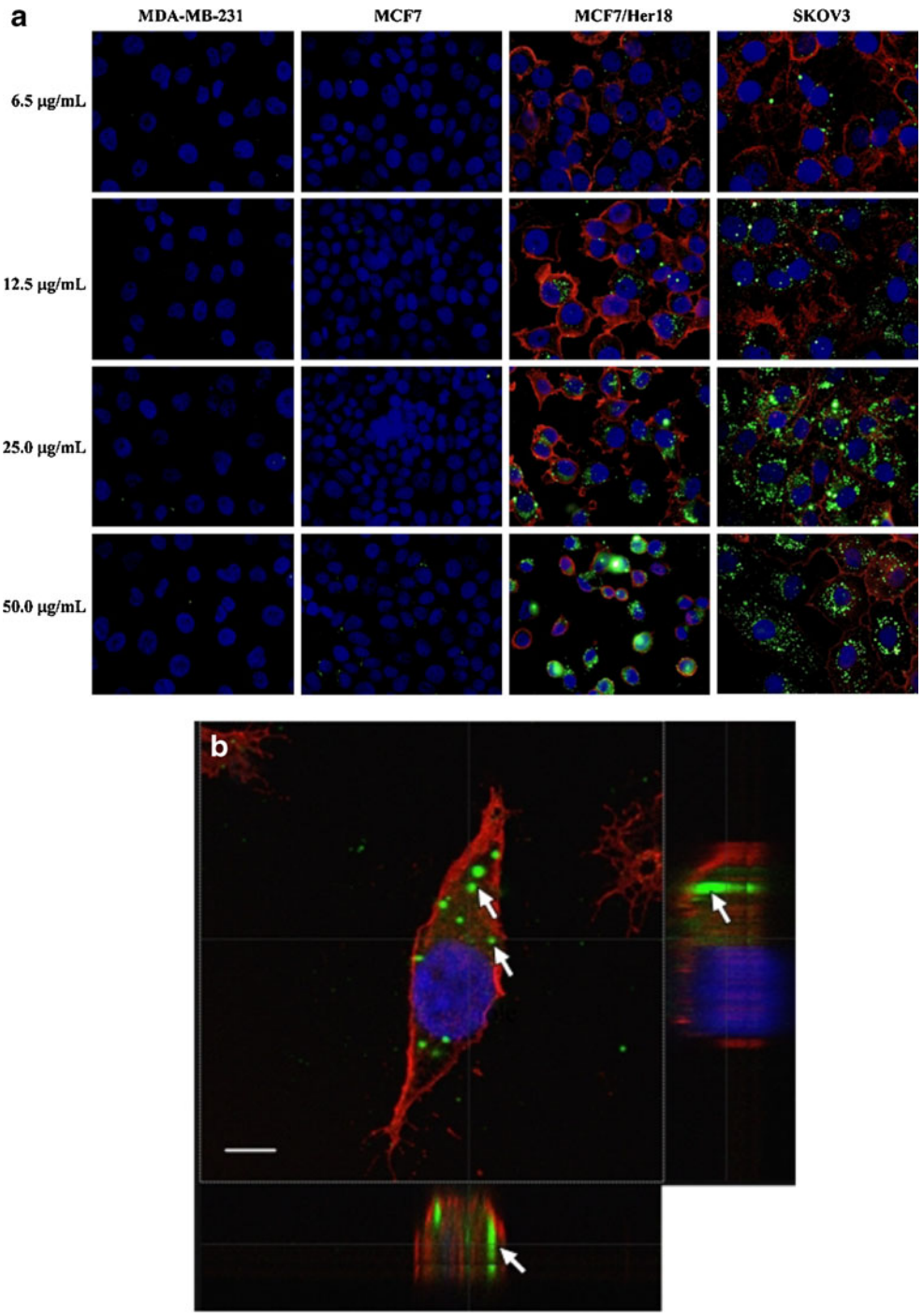

Fig. 5 Selective internalization of NOBs. NOBs were assembled with Cal-ZH2 and encapsulated with 1 μg/ml yellow GGK dye. The resulting NOBs (*green*) were added to 1×10^5 cells to reach the indicated concentration (shown on the *left*) and incubated for 2 h. After repeated washing for three times, cells were processed for further analyses. **a** Analysis by fluorescence microscopy. Cell nuclei (*blue*) and the HER2/*nue* receptor (*red*) were stained with DAPI and anti-HER2/*neu* antibody, respectively. Individual images were taken and then merged as shown on the right. **b** Analysis by confocal laser scanning microscopy (CLSM). After treated with Cal-ZH2-based NOBs, SKOV3 cells were analyzed by CLSM. *Insets*: Two three-dimensional reconstruction sections, including *X–Z* (*bottom*) and *Y–Z* (*right*) sections

lines used here were MDA-MB-231 (ovarian), SKOV3 (ovarian), MCF7 (breast), and MCF7/Her18 (HER2-transfected stable cell line). In essence, cell concentration was determined by a hemocytometer. For experiments, cells were seeded into 24-well plates at a cell density of 1×10^5 cells per well.

Fluorescence microscopy, confocal microscopy, and flow cytometry

Tumor cells were treated with dye-loaded NOBs and then prepared for further analyses as reported previously (Chiang et al. 2011). The anti-HER2/*neu* antibody (Santa

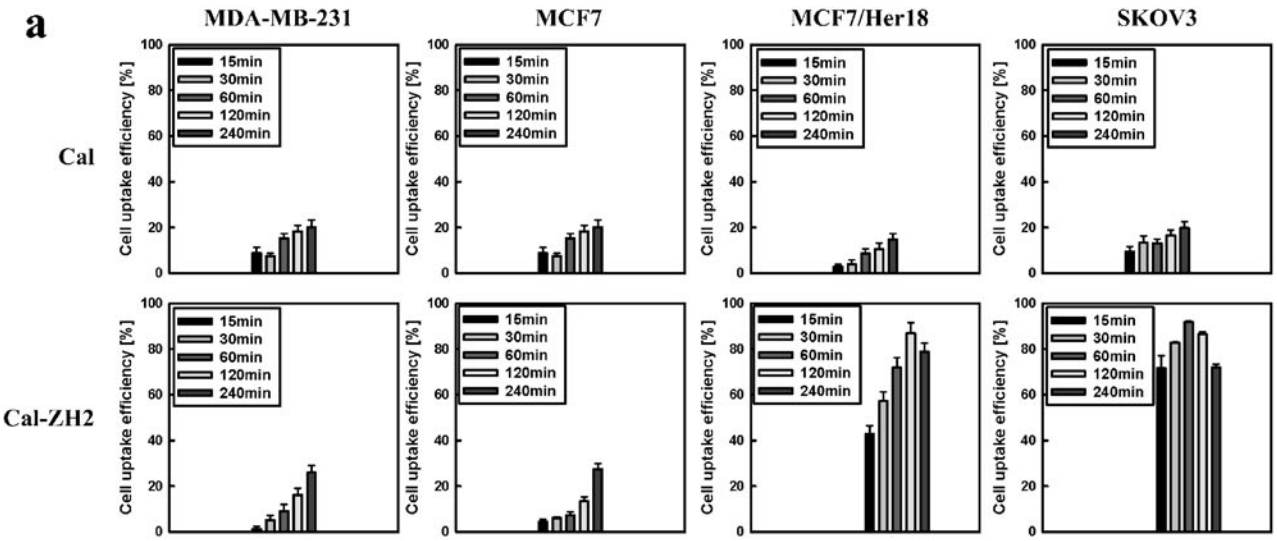

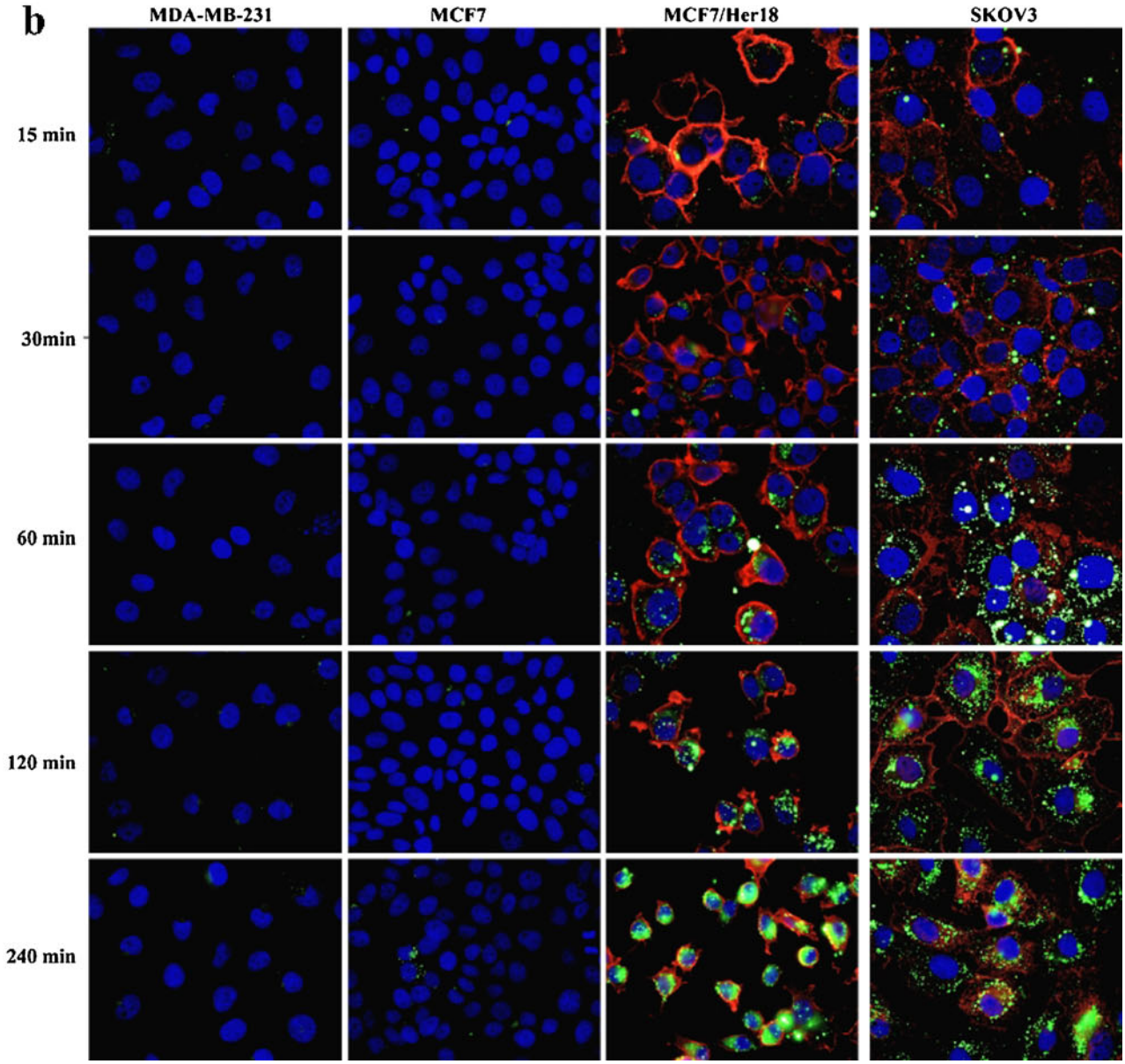

◀ **Fig. 6** Internalization efficiency of NOBs by flow cytometry and confocal microscopy. Refer to Fig. 5; cells were treated with Cal-based NOBs (*green*) at 25 μg/ml. **a** Analysis by flow cytometry. Various cells were exposed to ZH2-displayed (Cal-ZH2) or ZH2-lacking NOBs (Cal) for an indicated time. All experiments were conducted in triplicate. **b** Analysis by fluorescence microscopy. Incubation time was shown on the *left-hand side* of each panel

Cruz Biotech., USA) was applied to cells. After washing, anti-mouse IgG-TRIAC (Jackson ImmunoResearch Lab., USA) was administrated to stain cell membranes. Meanwhile, cell nuclei were stained with diamidino-2-phenylindole (DAPI) and rinsed with the sodium phosphate buffer. Both fluorescence microscopy (Olympus IX71, Japan) and confocal microscopy (Leica TCS SP2, Germany) were used to analyze the cells.

In addition, tumor cells were seeded to 6-well plate at a cell density of 1×10^5 cells/well. NOBs were then applied to cells for an indicated period of time. Followed by washing, cells were trypsinized and harvested for analyses using a FACScanto flow cytometer system (Becton Dickinson, USA).

In vitro assessment of dye release

The release profile of the yellow GGK dye from NOBs was determined following the reported protocol (Chiang et al. 2011). In brief, Cal-ZH2-based NOBs (1 ml) were placed in a dialysis bag (MW cut-off ranging from 12,000 to 14,000 Da) that was immersed in the buffer at 37°C with constant stirring. At time intervals, aliquots of the solution (100 μl) were withdrawn and the content of dye was measured by a spectrofluorometer (FP-6200; Jasco, Japan). The absorbance obtained was normalized to that with the initial content of the dye.

Results

Self-assembly of NOBs by Cal-ZH2

Production of Cal-ZH2 in *E. coli* was analyzed by SDS-PAGE (Fig. 1). Upon induction by IPTG, the bacterial strain was able to overproduce Cal-ZH2 in an insoluble form that was mainly present in the cell lysate (ppt-1). Self-assembly of NOBs was carried out by subjecting the mixture, containing olive oil, PLs, and isolated Cal-ZH2, to sonication. After centrifugation, NOBs sat on the top of mixture solution while no Cal-ZH2 was left in the supernatant fraction (sup-2) and the cell pellet part (ppt-2). NOBs were recovered and heated to liberate incorporated proteins. Consequently, Cal-ZH2 was identified as the main associated protein (NOB). This result indicates the strong association of Cal-ZH2 with oils. Similarly, Cal alone could be overproduced in *E. coli* receiving IPTG induction.

Modulation of Cal-ZH2-assembled NOBs

According to our previous study (Chiang et al. 2010), NOBs with a smaller size exhibited higher stability. Therefore, three factors affecting the size of NOBs were investigated in a systematic way. NOBs were first assembled with various plant oils at pH 7.5 by fixing the weight ratio of oil to Cla-ZH2 (O/P) at 1:1. As indicated in Fig. 2a, NOBs that were prepared from all types of oils except mineral oil exhibited a relatively small and homogenous size. The stability assay for NOBs also showed a similar trend (Fig. 3a).

At pH 7.5, NOBs were assembled using olive oil with various O/P ratios. Figures 2b and 3b show that lower O/P ratios gave a smaller size and higher stability of NOBs. In particular, NOBs had a small and compact morphology when the O/P ratio was lower than 1.

Finally, the effect of pH on NOB morphology was examined with the O/P ratio set at 1:1. NOBs tended to have a larger size and lower stability at pH lower than 7 (Figs. 2c and 3c). This is in agreement with our previous findings (Chiang et al. 2011). In contrast, NOBs had a smaller size and higher stability at an alkali condition. As further analyzed, NOBs assumed a spherical shape with the size ranging from 150 to 200 nm by AFM (Fig. 4), and their zeta potential was estimated to be −49.1 ±2.3 mV.

Selective internalization of Cal-ZH2-assembled NOBs

The functionality of ZH2 displayed on Cal-based NOBs was further investigated. To clearly illustrate, a hydrophobic fluorescence dye was encapsulated into NOBs with or without ZH2. Upon administration of the fluorescent dye-loaded NOBs, strong fluorescent signals could be detected in HER2/*neu*-postive cells (e.g., MCF7/Her18 and SKOV3) and the signal intensity increased in a NOB dose-dependent manner (Fig. 5a). In contrast, the signal was absent for HER2/*neu*-negative cells (e.g., MCF7 and MDA-MB-231). Similarly, no fluorescence could be observed in any type of tumor cells that were exposed to NOBs free of ZH2 (data not shown). Overall, the results suggest the functional display of ZH2 via Cal onto the surface of NOBs. This, in turn, leads to the specific association of functionalized NOBs with HER2/*neu*-positive cells.

In addition, the localization of internalized NOBs was confirmed by confocal microscopy. Figure 5b shows that the fluorescent dye-loaded NOBs were located in the cytoplasm of HER2/*neu*-positive cells. It clearly indicates

the ability of functionalized NOBs to target and penetrate HER2/*neu*-positive cells.

Internalization efficiency of Cal-ZH2-assembled NOBs

The internalization efficiency of Cal-ZH2-assembled NOBs was calculated as the percentage of fluorescence-emitting cells in the whole cell population. After administration of fluorescence dye-loaded NOBs for various time intervals, tumor cells were processed for analyses by flow cytometry. As depicted in Fig. 6a, internalization efficiency of ZH2-displayed NOBs towards HER2/*neu*-positive cells generally increased with the longer administration time. The maximum internalization efficiency was more than 90% for SKOV3 and MCF7/Her18 cells upon administration of functionalized NOBs for 60 and 120 min, respectively. A similar observation could also be obtained with fluorescence microscopy (Fig. 6b).

Release of the cargo dye

As reported recently, Ole-based NOBs displaying ZH2 were internalized into tumor cells via the endosomal entry pathway (Chiang et al. 2011). The cargo dye was released as a result of the instability of Ole-based NOBs at an acidic condition. Therefore, it spurred us to investigate the control-and-release feature of NOBs assembled by Cal-ZH2. SKOV3 cells were then administrated with fluorescent dye-loaded NOBs (25 μg/ml) for 1 h. After washing, the fluorescent signals within cells were monitored by confocal microscopy along the time course. As shown in Fig. 7a, the signals in the cells faded with time. After 5 days, the fluorescent images in the cells were barely detectable. The result implies that the cargo dye is released from Cal-based NOBs and gradually decays within the cells.

Furthermore, the dialysis analysis was conducted to analyze the in vitro release profiles of the cargo dye from Cal-ZH2-assembled NOBs. Figure 7b shows that an initial burst release occurred at the first 6 h. The released cargo dye reached 55% at pH 6.5 and 40% at pH7.5. After that, the dye was released in a stable and slow way. This sustained and prolonged release curve resembles the typical profile as commonly reported for many drug delivery systems (Kim et al. 2007; Yang et al. 2002).

Discussion

Nanotechnology has transformed the medication method for treatment of diseases. Apparently, targeted therapy is an emerging technology that receives the most intensive study. In essence, the approach relies on a nanocarrier that delivers therapeutic agents to target cells. However, one pressing challenge is to overcome the technical difficulties in the robust formulation of hydrophobic drugs with nanocarriers. In this study, we have sought to Cal-based NOBs as an alternative nanocarrier. Self-assembled NOBs comprise a central oil core that is enveloped by a monolayer of Cal-bound lipid (Fig. 8). To make NOBs functional, the anti-HER2/*neu* motif (e.g., ZH2) was displayed at their surface by linkage to the C-terminus of Cal. It is known that HER2/*neu* belongs to the human epidermal growth factor receptor family (Hung and Lau 1999). An abnormal and uncontrolled expression of HER2/*neu* can eventually lead to the progression of many aggressive tumors (Citri and Yarden 2006). As illustrated, Cal-based NOBs with surface display of ZH2 could specifically penetrate HER2/*neu*-positive tumor cells (Fig. 5a and b). This indicates that fusion of Cal with the bioactive motif provides a simple and feasible way for functionalization of NOBs.

The translocation path of the HER2/*neu* receptor into cells was proposed previously (Giri et al. 2005). The receptor enters cells by the endocytic internalization and then interacts with importin, a transport protein. Escorted by the nuclear pore protein, HER2/*neu* travels to cell nucleus. In agreement with this proposed pathway, ZH2 on the surface of NOBs interacted with HER2/*neu* of tumor cells, leading to the internalization of NOBs into cell endosomes (Chiang et al. 2011). This translocation mechanism also resulted in the heterogeneous distribution of internalized NOBs in cells (Fig. 5b). Moreover, the internalization behavior of Cal-based NOBs was time-dependent (Fig. 6b), which is consistent with the invasion kinetics of anti-HER2/*neu* affibody-conjugated materials as reported (Alexis et al. 2008). At the acidic condition in cell endosomes (Ohkuma and Poole 1978; Yamashiro et al. 1983), NOBs started to disintegrate with the release of the cargo dye (Fig. 7a). Based on the in vitro assay, the release rate of cargo dyes from Cal-based NOBs is slower than that from Ole-based NOBs (Fig. 7b). After 7 h at pH 6.5, there was 55% cargo dyes being liberated for Cal-based NOBs whereas more than 90% was released for Ole-based NOBs (Chiang et al. 2011). The result implies the potential of Cal-based NOBs for the long-acting release system.

The size of Cal-based NOBs was tunable. As indicated in Fig. 2, the type of plant oils could affect the morphology of NOBs. This result suggests that Cal-ZH2 likely interacts differentially with various TAG compositions of oils. More Cal-ZH2 than oil in the formulation could result in smaller and more stable NOBs. It indicates that more terminal domains (bearing a negative charge) of Cal could contribute stronger repulsion force to maintain the integrity of NOBs. However, under an acidic condition, the electronegative

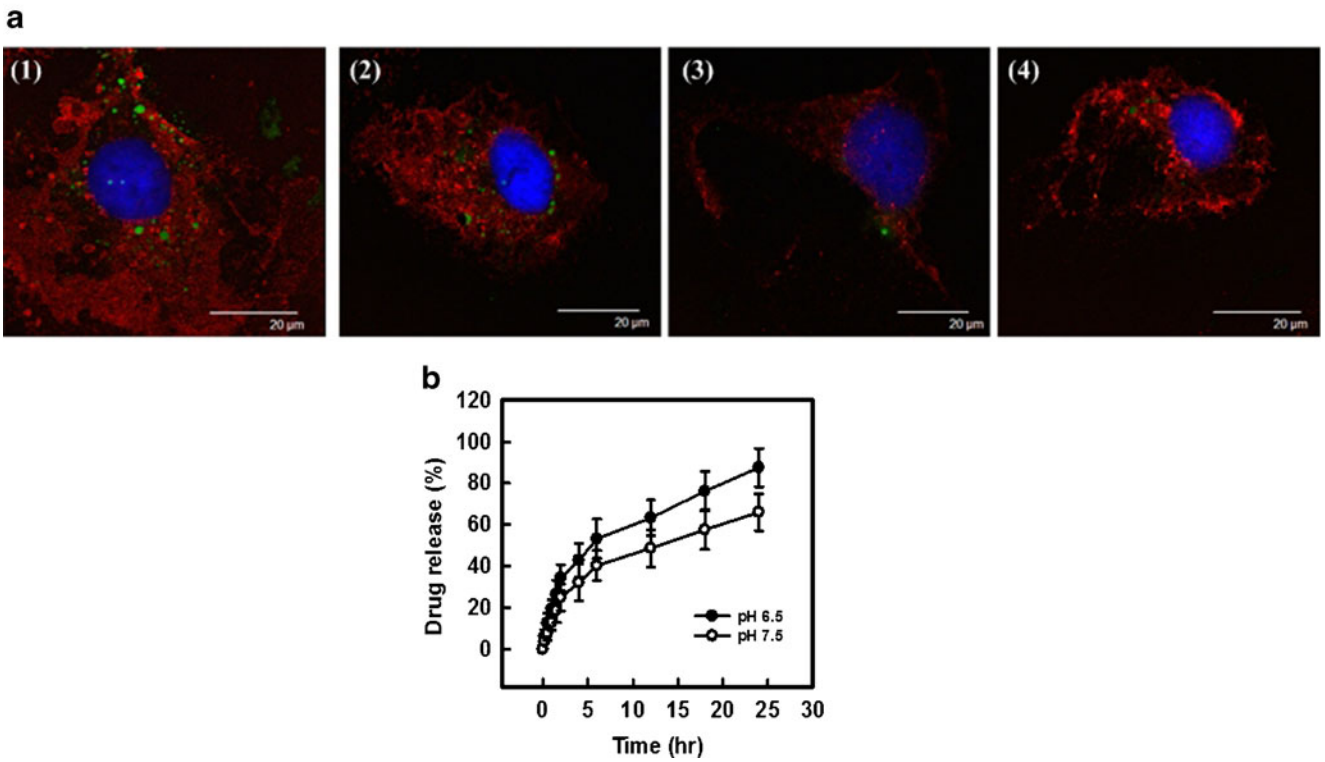

Fig. 7 Release of the fluorescence dye carried by NOBs. **a** Analysis by confocal microscopy. SKOV3 cells were treated with Cal-ZH2-based NOBs that carried the hydrophobic dye. The fluorescence emitted by internalized NOBs in the cells was analyzed by confocal microscopy on (*1*) day 0, (*2*) day 1, (*3*) day 3, and (*4*) day 5. **b** In vitro dye release profile. NOBs were loaded with the dye (6.25 μg/ml) and assessed for the dye release at pH 6.5 (*filled circle*) or pH 7.5 (*empty circle*) for 24 h. The experiment was conducted in triplicate

repulsion force is likely negated as a result of neutralization by H^+, which leads to coalescence of NOBs. The size of NOBs assembled by Cal can be tailored to reach less than 200 nm and is smaller than that with Ole (Chiang et al. 2011). In particular, the zeta potential of Cal-based NOBs (<−30 mV) was very high, suggesting that they are stable (Lee et al. 2007). Moreover, Cal-based NOBs is superior to Ole-based counterparts in terms of internalization efficiency (e.g., the percentage of fluorescence-emitting cells and incubation time) (Chiang et al. 2011). Regardless of the cell type, the uptake efficiency of Cal-based NOBs could reach above 90% with incubation time less than 2 h (Fig. 6a).

As well recognized, liposomes and polymeric micelles are two primary nanocarriers developed for a wide range of applications (Elbayoumi et al. 2007; Shmeedaa et al. 2009; Sugarman et al. 1996). Liposomes have a lipid-enclosed aqueous space that is not applicable for entrapment of water-repelling agents. Polymeric micelles contain a hydrophobic center surrounded by a hydrophilic shell and are effective for encapsulation of hydrophobic cargos. However, both carriers need to be conjugated with a functional ligand by a chemical modification before they can

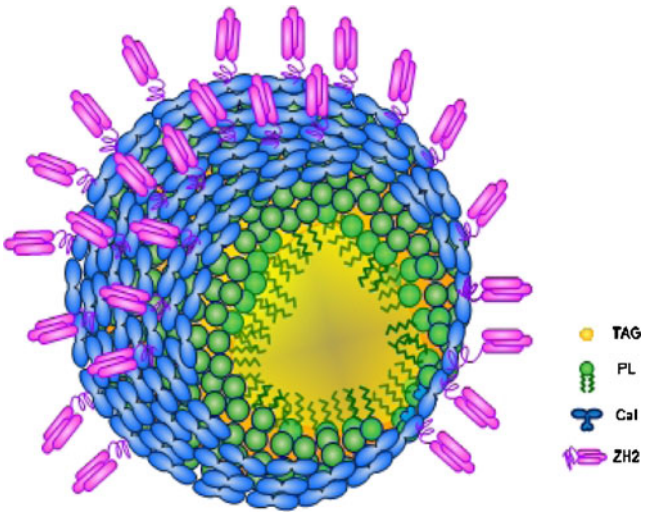

Fig. 8 A scheme illustrating the structure of Cal-ZH2-based NOBs. For clear illustration, a slice section of NOBs was removed to uncover the internal structure. Like plant OBs, NOBs are mainly composed of a TAG matrix enclosed by a monolayer of Cal-bound PLs. The ZH2 motif linked to Cal is displayed at the surface of NOBs, consequently leading NOBs to targeting HER2/*neu*-expressing tumor cells

selectively target tumor cells. In contrast, NOBs are oil droplets that facilitate the entrapment of hydrophobic agents. They are biocompatible and can be self-assembled in an easy and reproducible way. Simply fusing a bioactive motif with Cal can result in functional NOBs that are highly invasive and featured with an acid-triggered release nature. In conclusion, the advance of this novel approach may open a new avenue in the field of cancer nanotechnology.

Acknowledgements We like to acknowledge Instrument Center of R&D Office at China Medical University for technical assistance. This work was supported by National Science Council of Taiwan (NSC 99-2313-B-039-003-MY3, NSC 98-2221-E-035-029-MY3), China Medical University (CMU100-S-29), and Ministry of Economic Affairs (99-EC-17-A-10-S1-156).

References

Alexis F, Basto P, Levy-Nissenbaum E, Radovic-Moreno F, Zhang L, Pridgen E, Wang AZ, Marein SL, Westerhof K, Molnar LK, others (2008) HER-2-targeted nanoparticle-affibody bioconjugates for cancer therapy. ChemMedChem 3:1839–1843

Andresena TL, Jensenb SS, Jørgensen K (2005) Advanced strategies in liposomal cancer therapy: problems and prospects of active and tumor specific drug release. Prog Lipid Res 44:68–97

Chen JC, Tsai CC, Tzen JTC (1999) Cloning and secondary structure analysis of caleosin, a unique calcium-binding protein in oil bodies of plant seeds. Plant Cell Physiol 40:1079–1086

Chen MC, Chyan CL, Lee TT, Huang SH, Tzen JTC (2004) Constitution of stable artificial oil bodies with triacylglycerol, phospholipid, and caleosin. J Agric Food Chem 52:3982–3987

Chiang CJ, Chen HC, Chao YP, Tzen JTC (2005) Efficient system of artificial oil bodies for functional expression and purification of recombinant nattokinase in *Escherichia coli*. J Agric Food Chem 53:4799–4804

Chiang CJ, Chen HC, Kuo HF, Chao YP, Tzen JTC (2006) A simple and effective method to prepare immobilized enzymes using artificial oil bodies. Enzyme Microb Technol 39:1152–1158

Chiang CJ, Chen HC, Chao YP, Tzen JTC (2007) One-step purification of insoluble hydantoinase overproduced in *Escherichia coli*. Protein Expr Purif 52:14–18

Chiang CJ, Chern JT, Wang JY, Chao YP (2008) Facile immobilization of evolved *Agrobacterium radiobacter* carbamoylase with high thermal and oxidative stability. J Agri Food Chem 56:6348–6354

Chiang CJ, Chen CJ, Chang CH, Chao YP (2010) Selective delivery of cargo entities to tumor cells by nanoscale artificial oil bodies. J Agric Food Chem 58:11695–11702

Chiang CJ, Lin LJ, Lin CC, Chang CH, Chao YP (2011) Selective internalization of self-assembled artificial oil bodies by HER2/neu-positive cells. Nanotechnol 22:015102

Cho K, Wang X, Nie S, Chen Z, Shin DM (2008) Therapeutic nanoparticles for drug delivery in cancer. Clin Cancer Res 14:1310–1316

Citri A, Yarden Y (2006) EGF-ERBB signalling: towards the systems level. Nat Rev Mol Cell Biol 7:505–516

Cohen SN, Bernstein H (1996) Microparticulate systems for the delivery of proteins and vaccines. Marcel Dekker, New York

Elbayoumi TA, Pabba S, Roby A, Torchilin VP (2007) Antinucleosome antibody-modified liposomes and lipid-core micelles for tumor-targeted delivery of therapeutic and diagnostic agents. J Liposome Res 17:1–14

Farokhzad OC, Langer R (2009) Impact of nanotechnology on drug delivery. ACS Nano 3:16–20

Fernandez AM, Van Derpoorten K, Dasnois L, Lebtahi K, Dubois V, Lobl TJ, Gangwar S, Oliyai C, Lewis ER, Shochat D et al (2001) *N*-Succinyl-(β-alanyl-l-leucyl-l-alanyl-l-leucyl)doxorubicin: an extracellularly tumor-activated prodrug devoid of intravenous acute toxicity. J Med Chem 44:3750–3753

Frandsen GI, Mundy J, Tzen JTC (2001) Oil bodies and their associated proteins, oleosin and caleosin. Physiol Plant 112:301–307

Giri DK, Ali-Seyed M, Li LY, Lee DF, Ling P, Bartholomeusz G, Wang SC, Hung MC (2005) Endosomal transport of ErbB-2: mechanism for nuclear entry of the cell surface receptor. Mol Cell Biol 25:11005–11018

Huang AH (1996) Oleosins and oil bodies in seeds and other organs. Plant Physiol 110:1055–1061

Hung MC, Lau YK (1999) Basic science of HER2/*neu*: a review. Semin Oncol 26:51–59

Kim GY, Tyler BM, Tupper MM, Karp JM, Langer RS, Brem H, Cima MJ (2007) Resorbable polymer microchips releasing BCNU inhibit tumor growth in the rat 9 L flank model. J Control Release 123:172–178

Lee HK, Lee HY, Jeon JM (2007) Codeposition of micro- and nano-sized SiC particles in the nickel matrix composite coatings obtained by electroplating. Surf Coat Technol 201:4711–4717

Lipinski CA, Lombardo F, Dominy BW, Feeney PJ (2000) Experimental and computational approaches to estimate solubility and permeability in drug discovery and development settings. Adv Drug Deliv Rev 46:3–36

Liu TH, Chyan CL, Li FY, Tzen JTC (2009) Stability of artificial oil bodies constituted with recombinant caleosins. J Agri Food Chem 57:2308–2313

Miller JH (1972) Experiments in molecular genetics. Cold Spring Harbor Laboratory, Cold Spring Harbor

Napier JA, Stobart AK, Shewry PR (1996) The structure and biogenesis of plant oil bodies: the role of the ER membrane and the oleosin class of proteins. Plant Mol Biol 31:945–956

Ohkuma S, Poole B (1978) Fluorescence probe measurement of the intralysosomal pH in living cells and the perturbation of pH by various agents. Proc Natl Acad Sci U S A 75:3327–3331

Orlova A, Magnusson M, Eriksson TLJ, Nilsson M, Larsson B, Hoiden-Guthenberg I, Widstrom C, Carlsson J, Tolmachev V, Stahl S, others (2006) Tumor imaging using a picomolar affinity HER2 binding affibody molecule. Cancer Res 66:4339–4348

Peng CC, Lin IP, Lin CK, Tzen JTC (2003) Size and stability of reconstituted sesame oil bodies. Biotechnol Prog 19:1623–1626

Peng CC, Chen JCF, Shyu DJH, Chen MJ, Tzen JTC (2004) A system for purification of recombinant proteins in *Escherichia coli* via artificial oil bodies constituted with their oleosin-fused polypeptides. J Biotechnol 111:51–57

Shmeedaa H, Tzemacha D, Maka L, Gabizon A (2009) Her2-targeted pegylated liposomal doxorubicin: retention of target-specific binding and cytotoxicity after *in vivo* passage. J Control Release 136:155–160

Sugarman SM, Zou YY, Wasan K, Poirot K, Kumi R, Reddy S, Perez-Soler R (1996) Lipid-complexed camptothecin: formulation and initial biodistribution and antitumor activity studies. Cancer Chemother Pharmacol 37:531–538

Tai SSK, Chen MCM, Peng CC, Tzen JTC (2002) Gene family of oleosin isoforms in sesame seed oil bodies. Biosci Biotechnol Biochem 66:2146–2153

Torchilin VP (2005) Lipid-core micelles for targeted drug delivery. Curr Drug Deliv 2:319–327

Torchilin VP (2007) Micellar nanocarrier: pharmaceutical perspectives. Pharma Res 24:1–16

Tzen JTC, Huang AH (1992) Surface structure and properties of plant seed oil bodies. J Cell Biol 117:327–335

Tzen JTC, Lie GC, Huang AH (1992) Characterization of the charged components and their topology on the surface of plant seed oil bodies. J Biol Chem 267:15626–15634

Tzen JTC, Chuang RL, Chen JC, Wu LS (1998) Coexistence of both oleosin isoforms on the surface of seed oil bodies and their individual stabilization to the organelles. J Biochem 123:318–323

Yamashiro DJ, Fluss SR, Maxfield FR (1983) Acidification of endocytic vesicles by an ATP-dependent proton pump. J Cell Biol 97:929–934

Yang Z, Zhang Y, Markland P, Yang VC (2002) Poly(glutamic acid) poly(ethylene glycol) hydrogels prepared by photoinduced polymerization: synthesis, characterization, and preliminary release studies of protein drugs. J Biomed Mater Res 62:14–21

Zhang L, Chan JM, Gu FX, Rhee JW, Wang AZ, Radovic-Moreno AF, Alexis F, Langer R, Farokhzad OC (2008) Self-assembled lipid- polymer hybrid nanoparticles: a robust drug delivery platform. ACS Nano 2:1696–1702